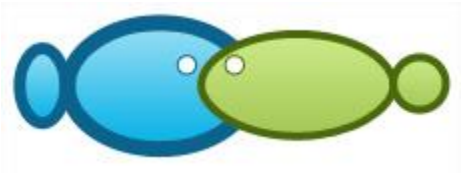

Evaluation of suitability of hydro-oceanographic characteristics for barramundi floating net cage aquaculture in Jepara Waters, Indonesia

[1]Amalia S. Ayuningtyas, [1]Agus A. D. Suryoputro, [1]Kunarso, [1]Muhammad Helmi, [2]Sapto P. Putro, [3]Kurnia Malik

[1] Department of Oceanography, Faculty of Fisheries and Marine Science, Diponegoro University, Tembalang, Semarang, Indonesia; [2] Department of Biology, Faculty of Science and Mathematics, Diponegoro University, Tembalang, Semarang, Indonesia; [3] Indonesian Navy Hydro-Oceanographic Center, Jakarta, Indonesia. Corresponding author: S. P. Putro, saptoputro@live.undip.ac.id

Abstract. Barramundi production in Indonesia continues to increase national income, yet its development is not optimal, thus research and development are required to support its growth. Based on previous studies, the quality of Jepara Waters is moderately suitable for aquaculture activities, with a good potential for aquaculture. However, the variances in conditions need to be evaluated before installing aquaculture. Variables used in this study include depth, ocean currents, waves, temperature, and salinity. Data was then evaluated spatially and temporally using the scoring method. Data sources for depth are taken from Hydro-Oceanographic Center, Indonesian Navy, for current and wave, data are taken from the results of 3D and 2D model data, while temperature and salinity data are from Marine Copernicus. The suitability evaluation area is split into four quadrants (A, B, C, D). The results showed that the most suitable locations to establish the aquaculture are in areas C and D, with a surface of 14,924.20 Ha (around 56.79% of the total research area), at a distance of 4.99–17.37 km from the coastline, with the most suitable time in January. Temperature, salinity, current, and wave data were validated using field data, and tidal modelling was validated using tidal data from the Geospatial Information Agency.
Key Words: 3D modelling, floating net cage, geographic information system, Jepara, MIKE.

Introduction. Indonesia's marine waters are used for fishing, exploration, and aquaculture purposes (Akrim et al 2019), with the objective of enhancing aquaculture production, which is critical to Indonesia's economic structure (Triarso & Putro 2019). According to FAO (2024), barramundi aquaculture production in Indonesia supplied more than 8.2% of global barramundi demand in 2018 and provided up to USD 200 million in state income in 2018, and it has been increasing every year for the last few decades. However, this industry is not yet optimal in Indonesia, thus research and development are required to support the expansion of this aquaculture sector (Irmawati et al 2021). Aquaculture with floating net cages is one method of aquaculture sustained by the environment itself (Cardia & Lovatelli 2015).

In this study several environmental parameters were evaluated to determine the suitability of water conditions, both for the structure of the cages and for the barramundi fish. The placement of floating net cages depends on the ecological condition of the waters. In addition, protection factors (currents and waves), water quality factors (temperature and salinity) and hydro-oceanographic data affect the cage mooring system and the water exchange, influencing the quality of life of cultured organisms and the pressure on the cage system. The parameters needed are depth, currents, waves, and water quality such as temperature and salinity. The required depth for placing net cages is between 10 and 50 m. The most important factors after depth, to be considered in making a cage mooring system are the currents and waves (Cardia & Lovatelli 2015). Current velocity has a strong effect on water exchange in the cage, feed distribution, ballast or moorings, rearing volume and net shape, monitoring operations by diving, as well as the distance from which solid

feed reduction is spread. The current and wave directly affect the mooring system of the cages and are related to the size of the seeds of the organisms to be cultivated. The form of cage is adapted to the water conditions and production needs (Cardia & Lovatelli 2015; Chu et al 2020; Bi et al 2020). An aquaculture environment where there is a lot of feed reduction or experiencing fouling can also increase the pressure force on the cage structure (Nobakht-Kolur et al 2021). In general, the minimum input for current speed requirements is 10–75 cm s^{-1} in order to determine the fixation system size for the mooring and elements to use. Furthermore, the significant wave height (Hs) is ≤3–4 m, for both tidal and coastal currents (Cardia & Lovatelli 2015). Then based on Indonesian National Standard for barramundi culture, the water quality will be classified as very suitable if the salinity is 15–35 ppt and the temperature is 26–32°C (Windarto et al 2019). Salinity influences feeding, feed conversion ratio, specific growth rate (SGR), and the immune system of cultivated fish. The water temperature plays a role in fish metabolism, tolerance to ammonia and carbon dioxide levels, and in managing fish stress (Cardia & Lovatelli 2015).

Based on previous research in 2021, the significant wave height (Hs) in the Jepara Awur Bay area is 0.50-1.73 m, the temperature is 21-26°C, and the salinity is 34-35 ppt; the average current speed is 0.01-0.421 m s^{-1} (Kurniawan et al 2021) and driven mostly by tidal or harmonic currents (Aziz et al 2019). Based on these findings, Jepara Waters offer a quality that is quite suitable for fish cultivation. However, because the water quality conditions in the Awur Bay Waters of Jepara are not representative for the whole research region, more research was needed to evaluate the status of water quality in other locations of Jepara Waters. Data collected in the current study is more reflective of the water quality for the floating net cages. Furthermore, the variable properties of each of these water areas differ, requiring an assessment of their eligibility for the installation of these aquacultures (Andayani et al 2018). The variables used for the evaluation of the suitability of the water characteristics consist of protection factors (depth, currents, and waves) and water quality factors (temperature and salinity). This assessment of the eligibility of water characteristics ignores the influence of residues formed by other ponds in the area of the waters, as well as the extreme fluctuations of the limiting factors.

To maintain the sustainability of current resources, it is vital to evaluate the suitability of hydro-oceanographic characteristics for aquaculture installation. Bad water quality, under d the floating net cage requirements, may cause problems in the surrounding ecosystem (Mulyono & Ritonga 2019) and may prevent fish adaptation and growth (Liu et al 2020; Wicaksono et al 2019). Furthermore, determining when and where to locate barramundi aquaculture in floating net cages is necessary for an optimal growth of barramundi.

Material and Method

Study sites. This research was conducted in Jepara Waters Figure 1. This study used a qualitative descriptive analysis method.

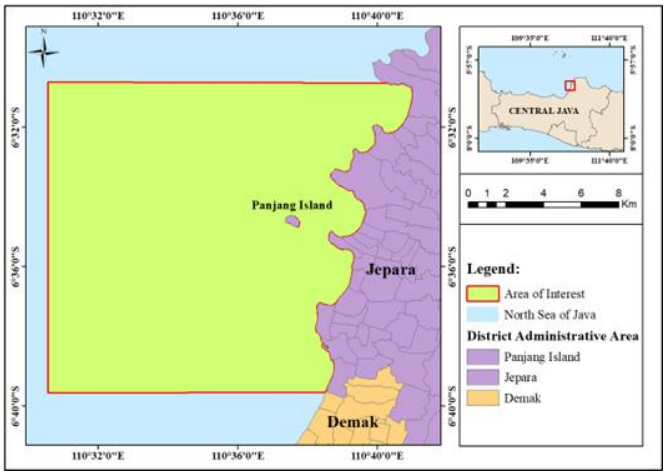

Figure 1. Area of interest: map of sampling in Jepara Waters.

The data used in this study consisted of primary and secondary data. Bathymetry, current speed, significant wave height, temperature, salinity, wind, and tide data were collected as primary data, while secondary data included Indonesian Rupa Bumi (RBI) maps of Jepara Regency, bathymetry from Hydro-Oceanographic Center, Indonesian Navy Maps, current speed and wave height from modelling, wind from CDS Copernicus, and temperature-salinity from Marine Copernicus.

Data sampling and preparation. Field data survey for primary data was used systematic random sampling approach by randomly identifying the first sampling point at one place, then selecting the next sampling point based on every 2-meter interval. Field data surveys were conducted for two days: in October 18th 2022, between 08:00 and 14:00 WIB and in October 19th, between 09:00 and 12:00 WIB. Temperature, salinity, and current data were taken at 33 sites, while wave and wind data were recorded near the dock, for 72 hours, starting in October 19th 2022 at 08:30 WIB. Tidal data was obtained from the Jepara tidal station. The primary data obtained was used to validate secondary data obtained from agencies, websites, and modelling. The wind data obtained has a resolution of 27.75 km grid^{-1} while temperature and salinity have a resolution of 9 km grid^{-1}. Wind, temperature, and salinity data were retrieved for a depth of 50 meters in January, April, July, and October to reflect the four seasons. Secondary data was processed by analyzing and interpreting bathymetry, temperature, and salinity data first. For each parameter the average value was calculated and interpolation curves were determined for the studied months. Temperature, salinity, wind, and tide data are used in 3D current modelling. Temperature and salinity data were downloaded and turned into 3D grid series data, while wind data was converted into time series data. Tidal data obtained from MIKE 21 toolbox tidal prediction data. Furthermore, all the data was entered for 3D flow modelling using the domain model with the Nesting method. The modelling generates 2D and 3D current models; the 2D model is used as raw data for 2D wave modelling. Primary data processing flow is shown in Figure 2.

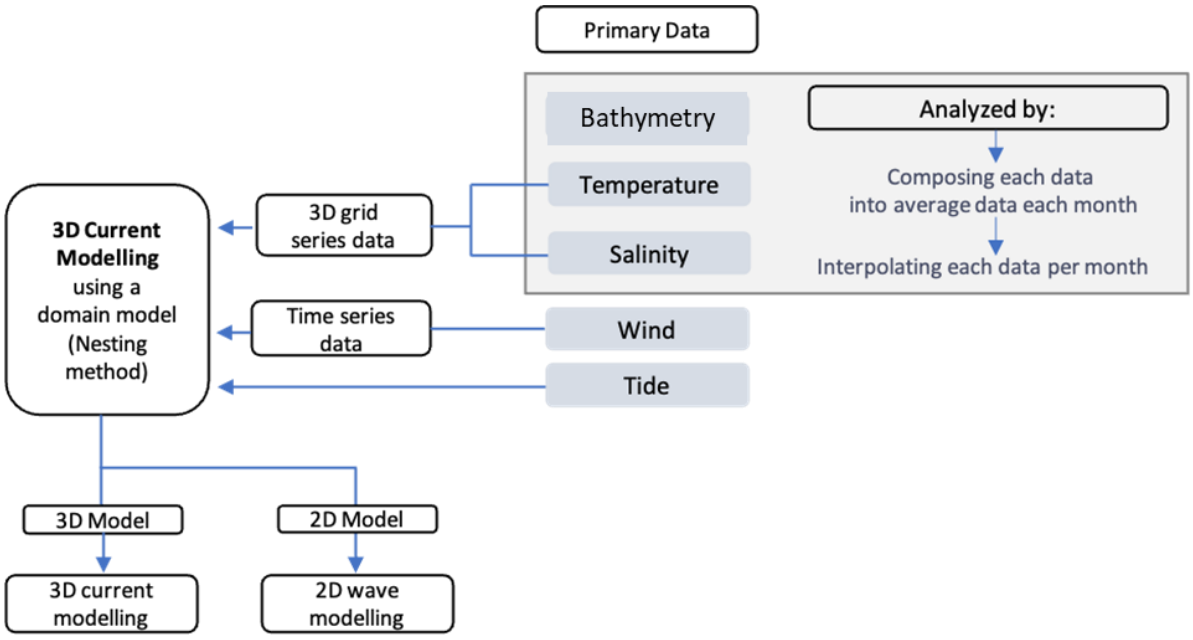

Figure 2. Primary data processing flowchart.

Model equations. Models are generated from MIKE software in 2D and 3D using different mathematical equations and module for each model; MIKE 21 Spectral Waves FM Module is used for the 2D wave model using a momentum equation in the x-axis and y-axis directions and a conservation of mass equation, while MIKE 3 Flow Model FM Module is used for the 3D ocean current model using the conservation of mass equation, the 3D Reynolds-averaged Navier-Stokes equations, which includes the effects of turbulent flow

and variable density, as well as the salinity and temperature, via their conservation equations. The 2D model is generated from the Cartesian coordinates system on the x-axis and y-axis while the 3D model uses the Cartesian coordinates system on the x-axis, y-axis, and z-axis (Irwan et al 2020; DHI 2017a). The 2D model input parameters are bathymetry, wind, and tide while the 3D model input parameters are bathymetry, temperature, salinity, wind, and tide. The outputs of 2D model are significant wave height, peak wave period, mean wave direction, surface elevation, current U velocity, current V velocity, wind speed, and wind direction. The outputs of 3D model are U velocity, V velocity, W velocity, current speed, current direction (horizontal), current direction (vertical), density, temperature, and salinity.
The 2D model's structure equations can be written as follows (DHI 2017b).

Conservation of mass equation:

$$\frac{\partial \zeta}{\partial t}+\frac{\partial p}{\partial x}+\frac{\partial q}{\partial y}=\frac{\partial d}{\partial t}$$

Momentum equations:
x-direction:

$$\frac{\partial p}{\partial t}+\frac{\partial}{\partial x}\left(\frac{p^2}{h}\right)+\frac{\partial}{\partial y}\left(\frac{pq}{h}\right)+gh\frac{\partial \zeta}{\partial x}+\frac{gp\sqrt{p^2+q^2}}{C^2.h^2}-\frac{1}{\rho_w}\left[\frac{\partial}{\partial x}(h\tau_{xx})+\frac{\partial}{\partial y}\left(h\tau_{xy}\right)\right]-\Omega_q-fVV_x+\frac{h}{\rho_w}\frac{\partial}{\partial x}(p_a)=0$$

y-direction:

$$\frac{\partial p}{\partial t}+\frac{\partial}{\partial y}\left(\frac{p^2}{h}\right)+\frac{\partial}{\partial x}\left(\frac{pq}{h}\right)+gh\frac{\partial \zeta}{\partial y}+\frac{gp\sqrt{p^2+q^2}}{C^2.h^2}-\frac{1}{\rho_w}\left[\frac{\partial}{\partial y}\left(h\tau_{yy}\right)+\frac{\partial}{\partial x}\left(h\tau_{xy}\right)\right]-\Omega_q-fVV_y+\frac{h}{\rho_w}\frac{\partial}{\partial xy}(p_a)=0$$

Where:
ζ (x,y,t) - the water level (m);
p (x,y,t) - the flux densities (kg m^{-3}) in x-axis directions in time, called uh;
q (x,y,t) - the flux densities (kg m^{-3}) in y-axis directions in time, called vh;
(u,v) in (uh,vh) - the depth-averaged speeds in x-axis and y-axis directions, respectively
d (x,y,t) - the time varying the water depth (m);
h (x,y,t) - the water depth (=ζ-d,m);
C(x,y) - the Chezy resistance ($m^{1/2}$ s^{-1});
g - the gravitational acceleration = 9.81 (m s^{-2});
f(V) - the friction factor of the wind;
V, V_x, V_y (x,y,t) - the wind speed and its components in x-axis and y-axis direction (m s^{-1});
Ω(x,y) - the latitude dependent (s^{-1}) Coriolis parameter;
p_a (x,y,t) - the atmospheric pressure (kg m^{-1} s^{-2});
ρ_w - the water density (kg m^{-3});
x,y - the space coordinates (m);
t - the time (s);
$\tau_{xx}, \tau_{xy}, \tau_{yy}$ - the components of effective shear stress.

Water level refers to the height of the water surface measured from a reference point, water depth is the actual value based on surface elevation and bathymetry, and time varying water depth is when the land is flooding also known as the elevation of tidal.

Then the equations used for three-dimensional modeling in MIKE 3 are expressed as follows (DHI 2017c):

$$\frac{1}{\rho c_s^2}\frac{\partial P}{\partial t}+\frac{\partial u_j}{\partial x_j}=SS$$

$$\frac{\partial u_i}{\partial t}+\frac{\partial\left(u_i u_j\right)}{\partial x_j}+2\Omega_{ij}u_j=-\frac{1}{\rho}\frac{\partial P}{\partial x_i}+g_i+\frac{\partial}{\partial x_j}\left(v_T\left\{\frac{\partial u_i}{\partial x_j}+\frac{\partial u_j}{\partial x_i}\right\}-\frac{2}{3}\delta_{ij}k\right)+u_i SS$$

$$\frac{\partial S}{\partial t}+\frac{\partial}{\partial x_j}\left(Su_j\right)=\frac{\partial}{\partial x_j}\left(D_s\frac{\partial S}{\partial x_j}\right)+SS$$

$$\frac{\partial T}{\partial t}+\frac{\partial}{\partial x_j}\left(Tu_j\right)=\frac{\partial}{\partial x_j}\left(D_T\frac{\partial T}{\partial x_j}\right)+SS$$

Where:
c_s - the seawater's sound speed;
ρ - the local density of the fluid;
u_i - the speed in the x_i-direction;
Ω_{ij} - the Coriolis tensor;
P - the pressure of fluid;
g_i - the vector of gravitational acceleration;
v_T - the turbulent eddy viscosity;
δ - the Kronecker's delta;
k - the turbulent kinetic energy;
T and S - the temperature and salinity;
D_s and D_T- the coefficients of the associated dispersion;
t - the time;
SS - the respective source-sink terms and thus differs from each equation.

MIKE 21 wind waves data are represented by the spectrum of wave action density N(σ,θ) variated in time and space (DHI 2017d). MIKE 21 spectral wave equilibrium equations can be expressed in spherical or Cartesian coordinates. The conservation equation for wave action in horizontal cartesian coordinates is expressed as follows (DHI 2017d).

$$\frac{\partial N}{\partial t}+\nabla\cdot(\vec{v}N)=\frac{S}{\sigma}$$

Where:
$N(\bar{x},\sigma,\theta,t)$ - the action density;
$\bar{x}=(x,y)$ - the Cartesian coordinates;
t - the time;
$\vec{v}=\left(c_x,c_y,c_\sigma,c_\theta\right)$ - the velocity of propagation of a wave group in $\bar{x},\sigma$ and θ;
$\bar{x}$ – the wave number vector with magnitude, x;
σ – the relative (intrinsic) angular frequency;
θ – the wave direction where a nautical convention is used (positive clockwise from true North);
S - the source term in the energy balance equation;
∇ - the divergence differential operator showing if a point is source or sink;
The conserved property is the density of action $\widehat{N}(\bar{x},\sigma,\theta,t)$ in spherical coordinates;
$\vec{x}=(\phi,\lambda)$ - the transformation of linear to spherical coordinates;
ϕ - the latitude;
λ - the longitude.

The density of action $\widehat{N}$ is related to the normal spectral density of action N and energy E by:

$$\widehat{N}=NR^2cos\phi=\frac{ER^2cos\phi}{\sigma}$$

Where:
R - the radius of the earth.
In spherical coordinates, the wave equilibrium equations are expressed as follows:

$$\frac{\partial \widehat{N}}{\partial t} + \frac{\partial}{\partial \phi} c_\phi \widehat{N} + \frac{\partial}{\partial \lambda} c_\lambda \widehat{N} + \frac{\partial}{\partial \sigma} c_\sigma \widehat{N} + \frac{\partial}{\partial \theta} c_\theta \widehat{N} = \frac{\hat{S}}{\sigma}$$

Where:
$\hat{S}(\bar{x}, \sigma, \theta, t) = SR2cos\phi$ - the total source and sink function (DHI 2017d).

The outputs of the 2D current and wave models are then mapped. The results of mapping data on depth, temperature, salinity, currents, and waves, as well as tidal time series data from the MIKE 21 toolbox, are then validated using field data and data from the Geospatial Information Agency. Data validation performed in accordance with the time and site of data collection, namely on October 18th at 08:00-14:00 WIB for temperature and salinity data, on October 19th at 09:00-12:00 WIB for current data and 72 hours after October 19th 2022 at 08:30 WIB for wave and wind data. The tidal data was validated hourly for each month (January, April, July, and October) using Jepara station tidal data from the Geospatial Information Agency. Data validation uses root mean squared error (RMSE) and mean absolute percentage error (MAPE). The RMSE validation was used for preliminary validation. If the value exceeded 1, then the validation was continued using MAPE to determine the level of tolerance at which the data can be used. RMSE is expressed by the following formula:

$$RMSE = \sqrt{\frac{\sum_{i=1}^{n} \left(x_{l,i} - x_{s,i}\right)^2}{n}}$$

Where:
$x_{l,i}$ - the data value of the Jepara Waters field;
$x_{s,i}$ - the data value from the results of secondary data processing;
n - the amount of the difference between the predicted and the model data.

MAPE is expressed by the following formula:

$$MAPE = \sum_{t=1}^{n} \frac{\left| \left| \frac{y_i - \hat{y}_i}{\hat{y}_i} \right| \times 100 \right|}{n}$$

Where:
$\hat{y}_i$ - the predicted or secondary data;
y_i - the data value of the Jepara Waters field or primary data;
n - the amount of data.

MAPE values were assigned one the four categories, from highly accurate to not accurate; highly accurate to marginally accurate shows that the data is valid, while not accurate shows that the data is not usable (Ali et al 2020). MAPE value category are shown in Table 1.

Table 1

MAPE values categories

No.	*MAPE value*	*Description*
1	<10%	Highly accurate data
2	10 – 20%	Good data
3	20 – 50%	Fairly good data
4	>50%	Inaccurate data

Furthermore, after being validated, each variable was assessed subjectively using the scoring technique based on previous research and modified. Each variable is given a score based on its weight, which will be summed up and assigned a relevant class. These

suitability class does not consider the influence of residues from other ponds in the region of the analyzed waters, neither the variable limiting factors for extreme events or the presence in lethal levels of substances affecting the water quality factors. Water suitability class for barramundi aquaculture in floating net cages, based on the protection and water quality factors, is shown in Table 2 and Table 3, respectively.

Table 2

Water suitability classes (protectability factor) for floating net cages

Variable	*Value*	*Suitable classes (score)*			*Source*
		Highly suitable/ S1 (Score: 3)	*Moderately suitable/ S2 (Score: 2)*	*Not suitable/ N (Score: 1)*	
Depth (m)	2.5	40.1-50	25.1-40	<25 and >50	Cardia & Lovatelli (2015)
Significant wave height (m)	3	1-2.5	2.6-4	>4 and <1	Cardia & Lovatelli (2015); Ariputro et al (2022)
Current speed (m^{-1})	2.5	0.51-0.75	0.1-0.5	>0.75 and <0.1	Cardia & Lovatelli (2015); Irmawati et al (2021)

Table 3

Water suitability classes (water quality factors) for floating net cages

Variable	*Value*	*Suitable classes (score)*			*Source*
		Highly suitable / S1 (Score: 3)	*Moderately suitable/S2 (Score: 2)*	*Not suitable/N (Score: 1)*	
Temperature (℃)	5	28.1-30	26-28 and 30.1-32	<26 and >32	Windarto et al (2019); Asdary et al (2019)
Salinity (ppt)	3	30.1-33	15-30 and 33.1-35	<15 and >35	Irmawati et al (2021); Windarto et al (2019); Asdary et al (2019)

Suitability classes for all parameters were assigned using the Equal Interval method. The interval value is obtained from the formula:

$$I = \frac{\sum(Bi \times Ni)max - \sum(Bi \times Ni)min}{k}$$

Where:
Bi - the value per parameter;
Ni - the suitability level (score);
I - the suitability class interval;
k - the number of suitability classes (highly suitable, moderately suitable, and not suitable).

This method divides the class interval into a preset number of suitability classes (Ariputro 2022). The suitability class is divided into three classes: Very Suitable (value interval 43.5-55.6), Moderately Suitable (value interval 30.9-43.2), and Less Suitable (value interval 18.5-30.8). The studied zone was divided into four quadrants (A, B, C, D), based on the distance from the shoreline (inshore or offshore), in order to assign them a suitability class (Figure 2).

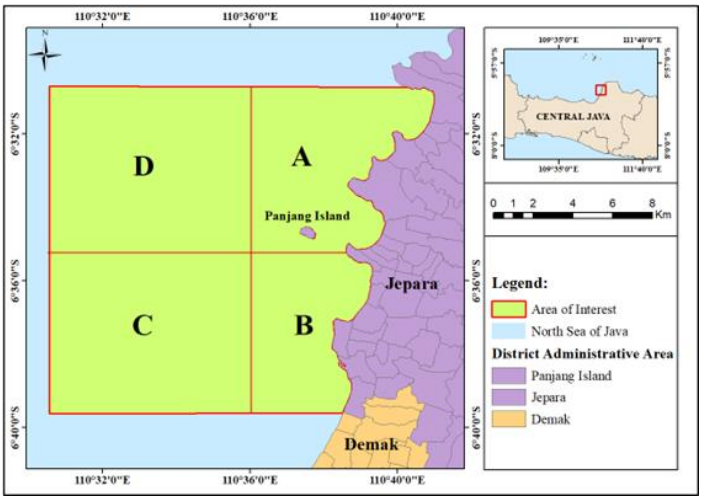

Figure 2. Division of analysis area suitability class classification.

Results and Discussion

Depth. Bathymetry or depth values in the Jepara Waters area are found to range from 0 to 40.20 m, based on the results (Figure 3). This depth value indicates that the study region is still in the mixed layer area. The characteristics of the current in the waters might be affected by the mixed layer. The wind that passes in the surface layer area continues to influence this layer. The depth in these waters, which ranges between 25 and 50 m, belongs to moderately suitable category and is ideal for barramundi aquaculture in floating net cages. This is due to the sediment concentration in the area around the cages being affected by water depth in relation to mean velocity and flow direction values. Areas C and D have depths ranging from 25 to 50 m. In addition, depth also affects cage structure, mooring design, and dive inspection for anchor conditions. The greater the water depth, the longer the mooring ropes for cages; a depth over 50 m will also require more equipment for mooring and professional anchor inspection. Shallow water depths have a higher potential for the spread of food waste particulates because the volume of cages is smaller. This condition has a higher potential for damage to fish stocks in the net (Cardia & Lovatelli 2015). Furthermore, water depth can affect survival and growth rate of the fish in growth phase: the smaller the water depth the higher the risk for disease and parasitic outbreaks. Another source stated that the water depth should be at least 39 m, to allow for submersion of the net enclosure and maximize the scopes of mooring. The areas with unconsolidated sediments are best for positioning anchors, while avoiding habitats in hard bottom, artificial reefs, areas of marine protected (MPAs), marine reserves, and Habitats of Particular Concern (HAPCs) (Fujita et al 2023).

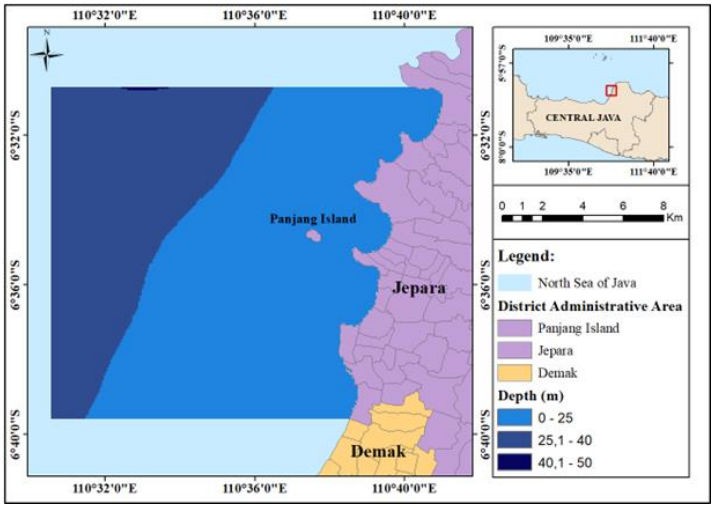

Figure 3. Depth distribution in Jepara Waters.

Temperature. Temperature recorded in Jepara Waters were ranging from 29.4 to 31.2°C (Figure 4). The temperature in January 2022 varies from 29.4 to 30.0°C; in April 2022 the temperature varies from 30.4 to 31.2°C; in July 2022, the temperature varies from 29.4 to 30.0°C and in October 2022, the temperature varies from 29.4 to 30.3°C. Most regions near the coast (A and B) have greater temperature than areas farther from the coast or in the open sea (C and D). Temporally, the highest range of water temperature values were recorded in April, followed by October and July, and the lowest range of water temperature were recorded in January. April is representative for the Transitional Season I, affected by the Western Season, when high precipitation increases freshwater mass influx into the waters; as a result, the temperature this month is warmer (Erfanda & Widagdo 2020). The temperature of Jepara Waters is within the optimal temperature range for barramundi growth. However, extreme circumstances can occur at any time. For example, if the water temperature exceeds 35°C, it might cause disease in the fish population (Irmawati et al 2021).

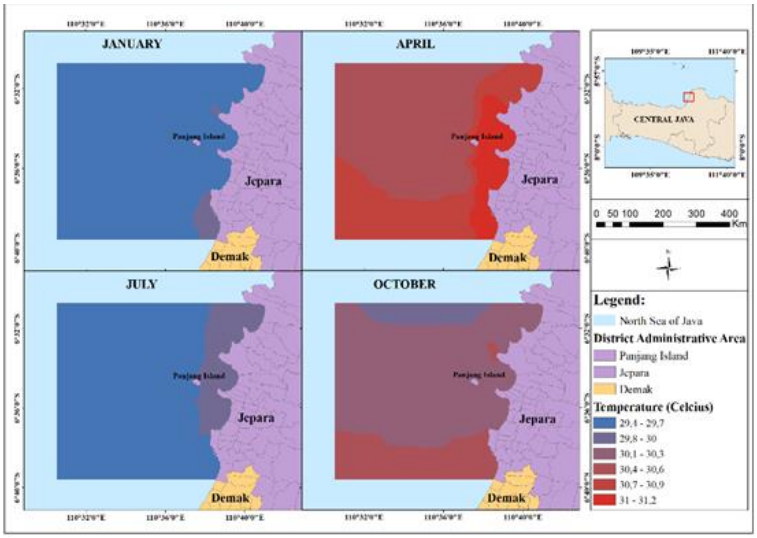

Figure 4. Monthly average temperature distribution in January, April, July, and October 2022 in Jepara Waters.

Salinity. The salinity values in the four months ranged from 31.4 to 32.9 ppt: from 31.4 to 33.2 ppt in January 2022, from 31.4 to 32.9 ppt in April 2022, from 31.4 to 32.6 ppt in July 2022 and from 32.1 to 32.9 ppt in October 2022 (Figure 5).

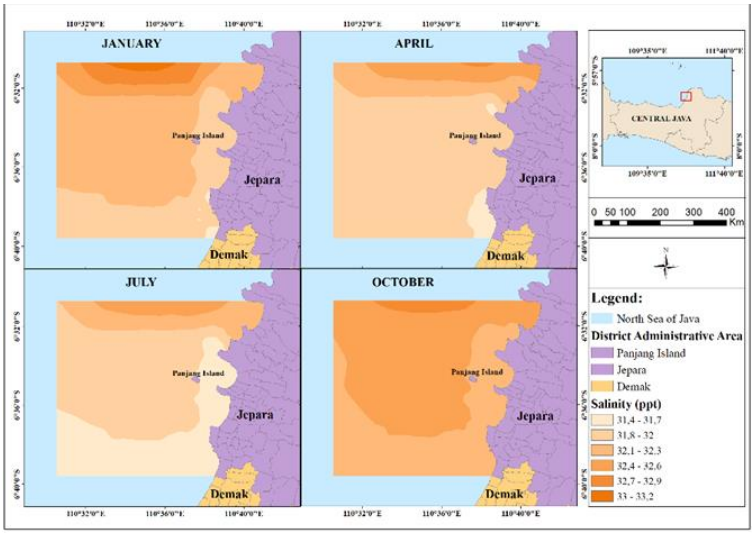

Figure 5. Monthly average salinity distribution in January, April, July, and October 2022 in Jepara Waters (Source: Marine Copernicus).

It can be seen that areas A and D have higher salinity values than areas B and C in all months. January has the highest range of water salinity values, followed by July, April, and October. October is representative of the Second Transitional Season, affected by the West Season. Because of the high rainfall in this month, at the beginning of the West Season, the salinity value is low (Erfanda & Widagdo 2020). The salinity range matches to the optimal salinity range for barramundi development, enlargement, and reproduction. However, extreme variables can occur at any time, and if the salinity value of the water is outside the range of 0-40 ppt, it can have an impact on fish, causing growth, enlargement, and reproduction abnormalities (Irmawati et al 2021).

Wind. The wind speeds in four months are varying from 1.8 to 11.2 m s^{-1} (Figure 6). Data processing shows that the wind in January mostly moves from the south with wind speed varying from 1.8 to 11.2 m s^{-1}, the wind in April comes from the north with speeds varying from 1.8 to 6.4 m s^{-1}, the wind in July comes from the northwest coast to the open sea with speeds varying in the range of 1.8 to 8.7 m s^{-1}, while the wind in October comes from the northwest with speeds varying from 1.8 to 6.4 m s^{-1}. The wind that rubs against the surface layer of the water will move the surface currents and waves in these waters (Cardia & Lovatelli 2015).

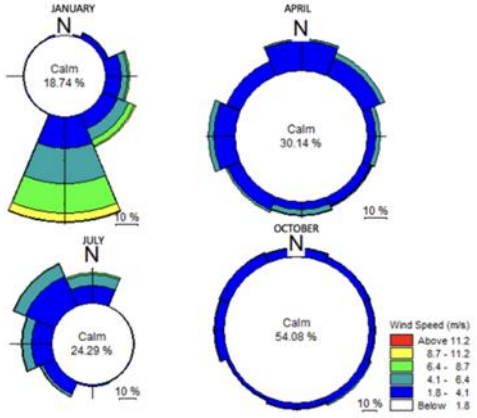

Figure 6. Monthly average wind speed distribution in January, April, July, and October 2022 in Jepara Waters (Source: CDS Copernicus).

Current. The minimum current velocity at an average depth in all months varied from 0 to 0.5 m s^{-1} (Figure 7b).

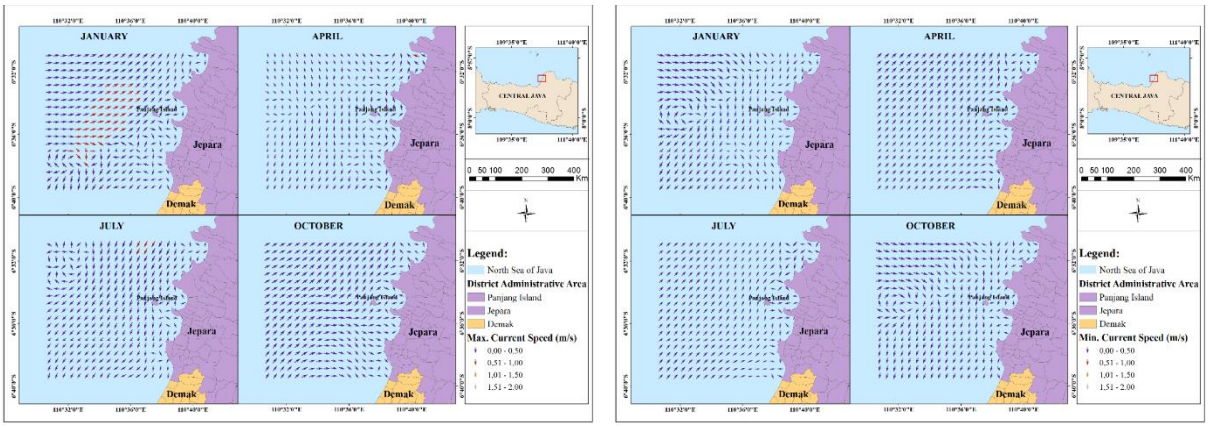

A B

Figure 7. Distribution of velocity and tidal current in January, April, July, and October 2022 in Jepara Waters. (A) Distribution of monthly maximum velocity and tidal current direction; (B) Distribution of monthly minimum velocity and tidal current direction (Source: Wind from CDS Copernicus, Temperature and Salinity from Marine Copernicus).

The maximum current speed value at the average depth in January, April, and July 2022 varied from 0 to 1.0 m s^{-1}, and in October 2022 it varied from 0 to 0.5 m s^{-1} (Figure 7a); according to the Norwegian Standard, it lies within the range of low to moderate site exposure. The value of current velocity is higher in areas C and D compared to A and B. Also, the range and distribution of the maximum current velocity values are higher in January, followed by July, April, and October. The value of current velocity decreases with increasing depth. The reduction in current speed is influenced by the force of contact with the seabed. Current speed and direction are also the effect of Wind, pressure differential in the water, topographic influences, and tidal forces.

The direction of the entire layer per depth reveals that the current moves in the same direction each month in both the horizontal and vertical plans (Figure 7): in the horizontal plan it moves towards the northeast and in the vertical direction it moves towards the east. The horizontal current direction indicates the movement of the surface layer and of each depth layer, driven by wind, whereas the vertical current direction indicates the displacement of each layer, driven by density differences (Figure 8). Due to the depth of the waters remaining in the mixed layer, wind and tides drive the currents, not density differences. At low tide, tidal currents can modify the stratification of the water column through density differences and profiles of vertical shear velocity. However, the data for these waters did not indicate any variations in currents due to differences in density, which may be a result of the aquatic system's well-mixed state (Pitchaikani & Bhaskaran 2019). The maximum water current velocity value range will determine the cage structure, feed dispersion, net shape and enlargement volume, diving monitoring activities, the dispersion distance of solid feed redistribution, and particularly the mooring system (Cardia & Lovatelli 2015).

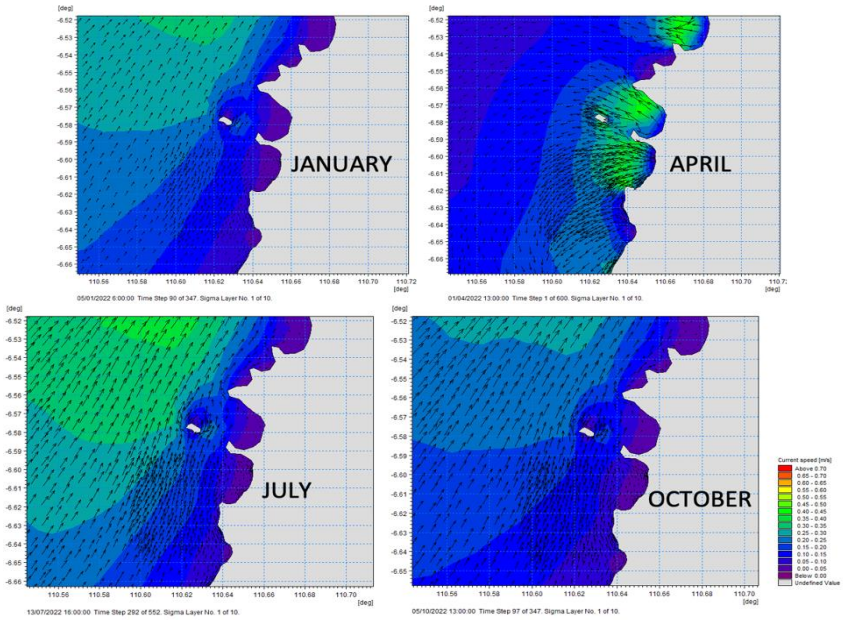

Figure 8. Map of monthly maximum velocity distribution and bottom layer tidal current direction in October 2022 in Jepara Waters (Source: Wind from CDS Copernicus, Temperature and Salinity from Marine Copernicus).

Wave. The maximum significant wave height values in January and July 2022 range from 0 to 2 m, while in April and October 2022 the values range from 0 to 1.5 m, with a peak wave period ranging from 2.4 to 11.5 seconds for each month (Figure 9). According to the Norwegian Standards (Cardia & Lovatelli 2015), significant wave height values fall within the "low" to "substantial" site exposure levels, and by period, values fall within the "moderate" to "extreme" site exposure levels. Significant wave height increases with the depth or distance from the shore. The highest values of significant wave height occur in the western and eastern seasons. The height and direction of significant waves can be influenced by the wind and implicitly by pressure differences (Erfanda & Widagdo 2020).

Significant wave height affects the total force, which impacts the strength and durability of the cage structure, especially the mooring system (Cardia & Lovatelli 2015). The durability and strength of a good mooring system will affect the efficiency and safety of the cage, and implicitly the productivity, so it is necessary to use for the mooring system materials that are customized for the value of significant wave height and current (Dong et al 2020).

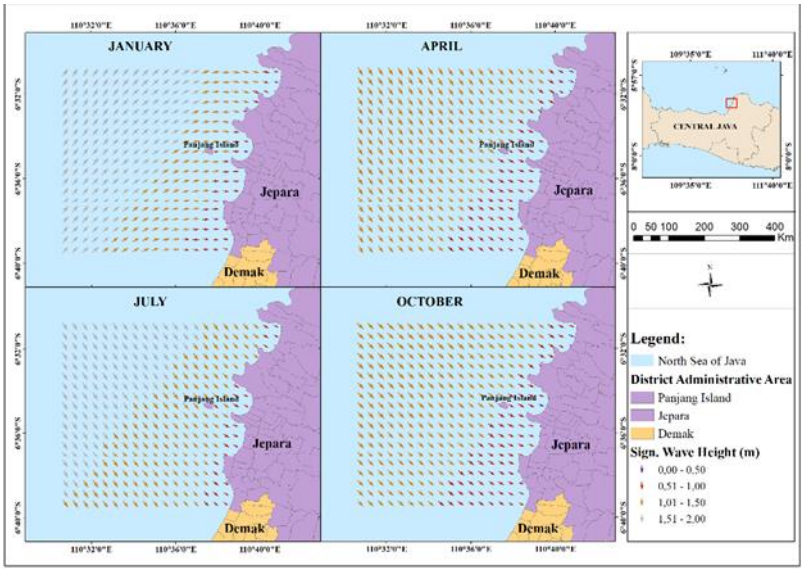

Figure 9. Distribution of monthly maximum significant height and wave direction in January, April, July, and October 2022 in Jepara Waters (Source: Wind from CDS Copernicus, Temperature and Salinity from Marine Copernicus).

Data validation. The RMSE values of depth, temperature, salinity, current speed, wave height, wind, and tide are calculated as follows: 1.55 for depth; 0.64 for temperature; 2.20 for salinity; 0.52 for current speed; 0.57 for wave height; 0.76 for wind; 0.55 for January tides; 0.62 for April tides; 0.67 for July tides; and 0.62 for October tides. The RMSE values for each month's temperature, current speed, wave height, wind, and tide parameters are low enough to be tolerated considering they are still within safe limits (nearly zero). However, the RMSE value for depth and salinity is greater than one, thus MAPE validation is required to evaluate the data's tolerance threshold. The MAPE calculation of the depth and salinity parameters is 22.47 and 7.32%, respectively. The MAPE validation value for the depth parameter is in the range of 20-50%, this indicates that the secondary depth data category is acceptable (Miraswan et al 2022; Wen et al 2022). The MAPE value for the salinity parameter is under 10% which indicates that secondary salinity data is valid (Miraswan et al 2022; Femiano et al 2022).

Water suitability. The suitability class processed per season aims to determine the best rearing period, from the time of spreading fish seeds until the harvesting time. The aquaculture process is also adjusted to the age of barramundi, where it takes six months for barramundi to reach harvestable size (Irmawati et al 2021). In January, it was determined that the „very suitable" zone is mainly located in areas C and D, with 14,924.20 ha, or approximately 56.79% of the total research area (Figure 10). In April, it is known that the „moderately suitable" zone has a surface, of 26,251.70 ha or around 99.90% of the total research area, while in July it is located in the areas C and D, with an area of 16,296.70 ha or approximately 60.02% of the total research area (Figure 10). In October, it was determined that the category of „moderately suitable" has the highest surface in areas A and D, with a combined surface of 24,686.30 ha or approximately 93.95% of the total research area (Figure 10). In the suitability class for all months, namely January, April, July, and October, the minimum current speed is the limiting factor for suitability. Aquaculture is most suitable in January 2022 in areas C and D, which are 4.99 to 17.37 km from the coast and comprise 14,924.20 ha, or approximately 56.79% of the entire study area.

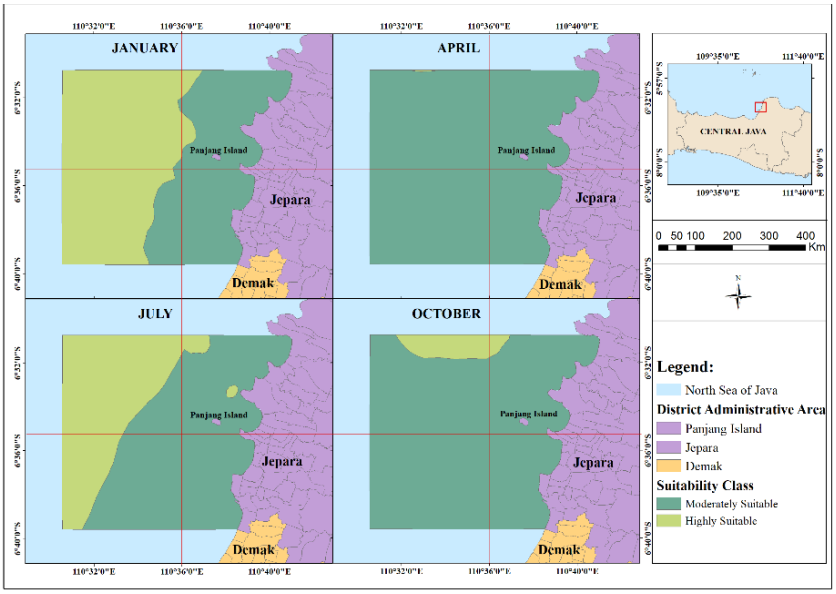

Figure 10. Distribution of water suitability classes for placement of barramundi aquaculture in floating net cages in January, April, July, and October 2022 in Jepara Waters.

Conclusions. The most suitable zone for aquaculture was located in the areas C and D, at a distance of 4.99-17.37 km from the coastline, and it was observed in January 2022. It covered 14,924.20 ha or about 56.79% of the entire study area. The characteristics were: depth ranging from 10 to 50 m, current speed ranging from 0 to 1.0 m s^{-1}, significant wave height ranging from 0 to 2 m, temperature ranging from 29.4 to 30.0°C, and salinity ranging from 31.4 to 33.2 ppt.

Acknowledgements. The authors would like to thanks to the Matching Fund Program Kedaireka, Faculty of Science and Mathematics, Diponegoro University in 2022 for involving the authors in surveys and data collection in the field. This study was financially supported by the scheme of Publication Research Grant (RPI)-Non-State Budget (Non-APBN), Contract No. 185-82/UN7.D2/PP/IV/2023.

Conflict of interest. The authors declare no conflict of interest.

References

Akrim D., Dirawan G. D., Rauf B. A., 2019 [Development of seaweed cultivation in improving the economy of coastal communities in Indonesia]. UNM Environmental Journals 2(2):52. [In Indonesian].

Ali A. M., Darvishzadeh R., Skidmore A., Gara T. W., O'Connor B., Roeoesli C., Heurich M., Paganini M., 2020 Comparing methods for mapping canopy chlorophyll content in a mixed mountain forest using Sentinel-2 data. International Journal of Applied Earth Observation and Geoinformation 87:1–14.

Andayani A., Hadie W., Sugama K., 2018 [Ecological carrying capacity for snapper cultivation in floating net cages, case study in Biak-Numfor Waters]. Jurnal Riset Akuakultur 13(2):179. [In Indonesian].

Ariputro A. B., Ismunarti D. H., Helmi M., 2022 [Integration of geospatial approaches and 2D hydrodynamic models for the suitability of grouper cultivation using floating net cages in the waters of Menjangan Besar Island, Karimunjawa Islands, Central Java Province]. Indonesian Journal of Oceanography 4(2):77–87. [In Indonesian].

Asdary M., Prastowo D., Yuliana, Kusumaningrum I., 2019 [Enlargement of white sea bass (*Lates calcalifer*) using a raceway recirculation system]. Jurnal Perekayasaan Budidaya Air Payau Dan Laut 14:1–7. [In Indonesian].

Aziz S. M., Rochaddi B., Handoyo G., Muslim M., Ismanto A., Setyono A., 2019 [Current patterns and distribution of bottom sediment in Jepara Waters]. Indonesian Journal of Oceanography 1(1):52–58. [In Indonesian].
Bi C. W., Zhao Y. P., Dong G. H., 2020 Experimental study on the effects of farmed fish on the hydrodynamic characteristics of the net cage. Aquaculture 524:1–9.
Cardia F., Lovatelli A., 2015 Aquaculture operations in floating HDPE cages. FAO Fisheries and Aquaculture Technical Paper, Rome, 176 p.
Chu Y. I., Wang C. M., Park J. C., Lader P. F., 2020 Review of cage and containment tank designs for offshore fish farming. Aquaculture 519:1–34.
Dong S., You X., Hu F., 2020 Effects of wave forces on knotless polyethylene and chain-link wire netting panels for marine aquaculture cages. Ocean Engineering 207:107368.
Erfanda A., Widagdo S., 2020 [Characteristics of meteo-oceanographic parameters and their influence on the distribution of salinity in the north and south waters of East Java]. Jurnal Riset Kelautan Tropis 2(1):1–15. [In Indonesian].
Femiano R., Werner C., Wilhelm M., Prisca E., 2022 Validation of open-source step-counting algorithms for wrist-worn tri-axial accelerometers in cardiovascular patients. Gait and Posture 92:206–211.
Fujita R., Brittingham P., Cao L., Froehlich H., Thompson M., Voorhees T., 2023 Toward an environmentally responsible offshore aquaculture industry in the United States: Ecological risks, remedies, and knowledge gaps. Marine Policy 147:105351.
Irmawati, Malina A. C., Alimuddin, Kadriah I. A. K., 2021 [Barramundi cultivation: Review of feasibility in floating net cages and traditional ponds]. Penerbit Nas Media Pustaka, Makassar, Indonesia, 119 p. [In Indonesian].
Irwan A., Wicaksono A., Khairin F. A., 2020 [Identification of sedimentation load distribution at DAM intake and hydroelectric reservoir (Case Study: Cirata Hydroelectric Power Plant, Purwakarta – West Java)]. Journal of Applied Science (Japps) 2(1):22–30. [In Indonesian].
Kurniawan H., Yulianto B., Riniatsih I., 2021 [The condition of seagrass fields in the waters of Jepara's Awur Bay is related to water environmental parameters and the presence of macro plastic waste]. Journal of Marine Research 10(1):29–38. [In Indonesian].
Liu H. F., Bi C. W., Zhao Y. P., 2020 Experimental and numerical study of the hydrodynamic characteristics of a semisubmersible aquaculture facility in waves. Ocean Engineering 214:1–13.
Miraswan K. J., Puspita W. A., Utami A. S., 2022 Prediction of the number of new cases of Covid-19 in Indonesia using fuzzy time series model chen. Sriwijaya Journal of Informatic and Applications 3(1):20–29.
Mulyono M., Ritonga L. B., 2019 [Aquaculture dictionary (Fisheries cultivation)]. STP Press, Jakarta, Indonesia, 188 p. [In Indonesian].
Nobakht-Kolur F., Zeinoddini M., Ghalebi A., 2021 Hydrodynamic forces in marine-fouled floating aquaculture cages: Physical modelling under irregular waves. Journal of Fluids and Structures 105:103331.
Pitchaikani J. S., Bhaskaran P. K., 2019 Tidal and non-tidal components of water level and currents in the Sundarbans ecosystem. SN Applied Sciences 1:1435–1444.
Triarso I., Putro S. P., 2019 [Development of sustainable productive aquaculture cultivation IMTA (Integrated Multi-Trophic Aquaculture) system (Case study in Karimunjawa Island, Jepara)]. Life Science 8(2):192–199. [In Indonesian].
Wen X., Jaxa-Rozen M., Trutnevyte E., 2022 Accuracy indicators for evaluating retrospective performance of energy system models. Applied Energy 325:1–15.
Wicaksono G. G., Restu I. W., Ernawati N. M., 2019 [Condition of the coral reef ecosystem in the western part of Pasir Putih Island, Sumberkima Village, Buleleng Regency, Bali Province]. Current Trends in Aquatic Science 2(1):37–45. [In Indonesian].
Windarto S., Hastuti S., Subandiyono R. A., Nugroho, Sarjito, 2019 [Growth performance of white snapper (*Lates calcarifer* Bloch, 1790) cultivated using a floating net cage system (FNC)]. Jurnal Sains Akuakultur Tropis 3(1):56–60. [In Indonesian].
*** DHI, 2017a MIKE 21 & MIKE 3 Flow model fm hydrodynamic and transport module scientific documentation. DHI headquarters, Denmark, 64 p.

*** DHI, 2017b MIKE 21 Flow model & MIKE 21 Flood screening tool hydrodynamic module scientific documentation. DHI headquarters, Denmark, 58 p.
*** DHI, 2017c MIKE 3 Flow model hydrodynamic module scientific documentation. DHI headquarters, Denmark, 69 p.
*** DHI, 2017d MIKE 21 spectral wave module scientific documentation. DHI headquarters, Denmark, 56 p.
*** FAO, 2024 *Lates calcarifer* Bloch, 1790. In: Fisheries and aquaculture. FAO, Rome, https://www.fao.org/fishery/en/aqspecies/3068/en.

Received: 22 June 2023. Accepted: 05 June 2024. Published online: 20 June 2024.
Authors:
Amalia Sekar Ayuningtyas, Department of Oceanography, Faculty of Fisheries and Marine Science, Diponegoro University, Tembalang, 50275 Semarang, Indonesia, e-mail: amaliasekar30@gmail.com
Agus Anugroho Dwi Suryoputro, Department of Oceanography, Faculty of Fisheries and Marine Science, Diponegoro University, Tembalang, 50275 Semarang, Indonesia, e-mail: agusanugroho@lecturer.undip.ac.id
Kunarso, Department of Oceanography, Faculty of Fisheries and Marine Science, Diponegoro University, Tembalang, 50275 Semarang, Indonesia, e-mail: kunarsosmg@gmail.com
Muhammad Helmi, Department of Oceanography, Faculty of Fisheries and Marine Science, Diponegoro University, Tembalang, 50275 Semarang, Indonesia, e-mail: mhelmi@lecturer.undip.ac.id
Sapto Purnomo Putro, Department of Biology, Faculty of Science and Mathematics, Diponegoro University, Tembalang, 50275 Semarang, Indonesia, e-mail: saptoputro@live.undip.ac.id
Kurnia Malik, Indonesian Navy Hydro-Oceanographic Center, 14430 Jakarta, Indonesia, e-mail: kurnia.malik@gmail.com

How to cite this article:
Ayuningtyas A. S., Suryoputro A. A. D., Kunarso, Helmi M., Putro S. P., Malik K., 2024 Evaluation of suitability of hydro-oceanographic characteristics for barramundi floating net cage aquaculture in Jepara Waters, Indonesia. AACL Bioflux 17(3):1075-1089.